International Journal of ChemTech Research
CODEN (USA): IJCRGG ISSN: 0974-4290
Vol.8, No.2, pp 829-835, 2015

Structural Explorations of Microwave Assisted Nanocrystalline Ceria Synthesis

P. Suriakala[1], K.Tamilarasan[2] and M.Kanagasabapathy[3]

[1]Department of Physics, Rajapalayam Rajus' College, Rajapalayam, Tamil Nadu, India.
[2]Department of Physics, Kongu Engineering College, Erode, Tamil Nadu, India
[3]Department of Chemistry, Rajapalayam Rajus' College, Rajapalayam, Tamilnadu, India

Abstract: Microwave induced combustion method was employed for the preparation of nickel mixed ceria nanocrystalline powder using cerium nitrate, nickel nitrate, glycine and sorbitol. Subsequently, three different molar composition of cerium nitrate was mixed with constant proportion of nickel nitrate, glycine and sorbitol to synthesis three samples. The resultant samples were analysed for structural, morphological and spectral characteristics using XRD, SEM, TEM, FTIR and UV-Vis spectroscopy. The crystallite sizes were about in the nano range of 27nm, 5nm & 4nm. There was a decrease in lattice parameter in the order of 5.4089A˚, 5.3921A˚ & 5.4014A˚. Degree of lattice distortion depends on NiO content in the ceria lattice. The FTIR spectrum shows the existence of groups such as $–NO_2$, –OH and C–H due to the solubility of nickel material. The absorption band is extended up to visible region in UV-Vis spectrum due to the substitution of Ni ion.
Keywords: Microwave, Optical properties, nanocrystalline materials, SEM, XRD.

Introduction:

The daunting task of saving world today is, from environmental pollutions and energy scarcity. The research in nanomaterials takes on different dimensions to fulfill the needs. Idealistic properties of nanocrystalline ceria based materials are used to solve and save this world in progressive way. The tallying of materials into ceria will push the boundaries and creating, huge booming properties like ionic, optical, structural, electronic, catalytic and magnetic properties [1-3], and vast applications such as solid oxide fuel cells, water gas shift reactions, oxygen sensor, and three way catalysts [4-7]. The structural, textural, and dynamic oxygen storage/release behaviours of $Ni_{0.1}Ce_{0.9}O_x$ are investigated [8]. The dynamic oxygen storage capacity and rate are largely promoted by Ni doping, and the thermal stability of the sample is also enhanced. The introduction of Ni into ceria mixed oxides strongly modifies the structural and textural properties, which influence the kinetics of bulk oxygen diffusion. A novel type of Ni-doped hierarchical nanostructured peony-like ceria (PCO) has been prepared and its catalytic activity is investigated and compared with that of Ni-loaded samples [9]. The doped ceria may also use for applications in controlling the air-to-fuel ratio in automobile exhaust [10]. Chlorinated hydrocarbons are hazardous pollutants which may convert into value added products with the help of Ni/CeO_2 using catalytic hydro-dechlorination technology [11]. Nickel is widely considered as an attractive material for SOFC anodes because it has good electronic conduction as well as catalytic activity for the electrochemical oxidation of hydrogen [12].

Ceria either in pure form or doped with other metals like Cu, and Ni, has a wide range of applications [13]. Incorporation of ceria particles into the Ni matrix was found to improve the corrosion resistance of pure Ni coatings [14]. Doughnut like structure CeNiO was prepared by a novel oxalate gel co-precipitation method [15]. The addition of Co, Ni, Cu, V and Fe into the ceria based anode material is found to have a considerable

effect on the morphology of the powders was reported [16]. Pure and transition metal doped ceria was prepared by flame synthesis [17]. Mesoporous $Ni_{nx}Ce_{1-x}O_n$ (x = 0.05, 0.13, 0.2) was also synthesized for use in the methane steam reforming reactions by reverse precipitation method [18]. The multifunctional material of Nickel mixed Ceria were prepared by microwave induced combustion process and studied their structural properties in this present work.

Experimental Procedure:

All the reagents used for the preparation were of analytical grade. Chemicals like Cerium Nitrate $Ce(NO_3)_3.6H_2O$ and Nickel Nitrate $Ni(NO_3)_2.6H_2O$ act as precursor materials and Glycine and Sorbitol act as a fuel. All the solutions were prepared by using doubly distilled water. The stock solution of 0.25M, 0.5M and 0.75M of $Ce(NO_3)_3.6H_2O$ and 0.25M of $Ni(NO_3)_2.6H_2O$ were prepared in advance and stored at room temperature. 100ml of $Ce(NO_3)_3.6H_2O$,100ml of $Ni(NO_3)_2.6H_2O$, 4ml of Glycine and 4ml of Sorbitol were mixed in the beaker. The mixed solution was heated at 250˚C for 10min and applied microwave power at 300W for 8min. During this process lot of fumes were observed. The process was incorporated for three different composition of cerium nitrate mixed with nickel nitrate to produce three different products. The details of the experimental procedure are shown in Table 1.

Table 1 Preparation details of nickel doped ceria

S.NO	Stock Solution mixed with 100ml of water			Mixture Taken	Microwave Oven	Final product
	1	2	3			
1	**10.85gm** of $Ce(NO_3)_3.6H_2O$	**7.3gm** of $Ni(NO_3)_2.6H_2O$	3.75 gm of Glycine	10ml of Cerium Nitrate + 10ml of Nickel Nitrate+ 0.4ml of Glycine + 0.4ml of Sorbitol	250°C 10min and 300W 8min	CNA
2	**21.7gm** of $Ce(NO_3)_3.6H_2O$					CNB
3	**32.5gm** of $Ce(NO_3)_3.6H_2O$					CNC

The X-ray diffraction (XRD) patterns of the powder samples were measured at room temperature with Bruker Axs Ds Advance diffractrometer with CuKα radiation of wavelength 1.5418 Å. Molecular structure and bonding characteristics were analyzed using FTIR (Thermo Nicolet, Avatar 370). Optical properties of Nickel doped ceria powder were explored by UV-Vis – NIR Spectrophotometer (Varian, Cary 5000). Surface morphology of the powders was studied using Scanning Electron Microscope JEOL Model JSM - 6390LV EDS JEOL Model JED – 2300 and TEM JEOL JEM 2100 High Resolution Transmission Electron Microscope (HRTEM) were used for morphology of the material.

Results and Discussion:

The ratio of fuel to nitrate in initial mixture, incident microwave radiation power and reaction time entail an immense pressure on characteristics of synthesized crystallites [19,20]. Here the amount of fuel, microwave power and reaction time were fixed constant for various compositions of mixed metal nitrates. Lower concentration of cerium nitrate mixed nickel nitrate with constant amount of fuel induced increase in reaction temperature which therefore increases the growth of the crystallites. During preparation, a sudden explosion taken place due to faster rate reaction and high reaction temperatures. As a consequence, a milder reaction between higher concentration of cerium nitrate and fuel resulting in lower reaction temperature was taken place and further to produce smaller and well defined crystallite. The heating rate of the reaction was the important parameter which depends on solubility of metal nitrates, fuel ratio and microwave power. Milder reaction affects nucleation rate. The main benefit of the introduction of microwaves into the reaction system is in obtaining a tremendously quick kinetic for crystallization, which may be ascribed to the controlled superheating of the solutions under microwave heating.

Fig.1 shows XRD patterns of nickel mixed ceria powder prepared by microwave combustion method. All samples show that there was an occurrence of polycrystalline peaks with moderate intensity. All the peaks were indexed based on a face centre cubic crystal fluorite type as ceria peaks (cf. JCPDS #34-0394). The powder prepared using the low concentrated Cerium Nitrate (0.25M - denoted as CNA) has lesser peak

broadening with high intensity in comparison to other two compounds designated as CNB and CNC. The XRD pattern contains ceria peaks and in addition some intensity peaks were observed at 2θ values of 36.941˚, 42.960˚ and 62.565˚. The additional peaks were identified and indexed for cubic NiO as (111), (200) and (220) planes as JCPDF #47-1049. Whereas the powders prepared using other two high concentrations (0.5M and 0.75M) of cerium nitrate shows broadened peaks and indexed for ceria only.

The peaks were considerably broader due to the smaller crystallite size and perhaps contribution from lattice microstrain. Strain- and size-related contributions are different functions of the diffraction angle [21], so that at least in principle, it should be possible to distinguish between the two effects. The Lorenztian peak shape function was used to fit diffraction profiles and extract the peak position, FWHM. We have estimated the average crystallite size (Dv) as by applying the Scherrer formula [22].

The accurate two theta positions of the powder samples were derived from the lorenztian peak fit. The lattice parameter of the Ni-doped ceria and NiO phases were calculated from their two theta positions using UNITCELL code [23] based on least square minimization method with zero shift refinement. The calculated lattice parameter and unit cell volumes of the samples were listed in Table.2. The lattice parameter values of CNA, CNB and CNC samples differ from the pure ceria lattice parameter of 5.4113 A˚ (1) [24] and found to be decreased. The unit cell volume of CNA, CNB and CNC values also decreased in comparison with pure ceria (158.4545Å^3). The variation of lattice dimension and unit cell volume changes may be attributed by the different atomic radii of Ni and Ce are 0.135nm and 0.185nm respectively. In addition the Ni substitution into the Ce lattice position may results the creation of cationic vacancies in the ceria lattice. In CNA, the Ni/Ce ratio is higher than that of the other two compositions namely CNB and CNC. Due to high amount of Ni in this composition, the Ni solubility limit in ceria exceeds, results the segregation of NiO observed in CNA. Even though some amount of Ni already in the Ceria lattice, results the shrinkage of the lattice change was observed. In another study suggest that the limit of solubility of Ni in ceria is in the range of 10 to 12% [25]. In CNB and CNC due to the lower Ni/Ce ratio, Ni doped ceria lattice was observed with relatively lower lattice distortion.

Table 2 XRD parameter of Nickel doped nanocrystalline ceria

sample	2θ (deg)	(hkl)	FWHM (deg)	Phase	Crystallite Size (nm)	Lattice parameter (A˚)	Unit cell volume (Å^3)
CNA	28.269 32.792 47.205 56.079 58.829 69.178 76.487 78.875	111 200 220 311 222 400 331 420	0.35418 0.33941 0.38566 0.38552 0.38421 0.40698 0.43867 0.41823	CeO_2	~27 (CeO_2)	5.4089 (1) (CeO_2)* 5.4113(1)	158.24 (1) 158.4545 *
	36.941 42.960 62.565	111 200 220	0.50323 0.60338 0.63218	NiO	~17 (NiO)	4.2046(2) (NiO)	74.33(1)
CNB	28.2193 32.3607 47.1096 56.0507 69.099	111 200 220 311 400	1.5082 1.7103 1.6138 1.6147 2.3086	CeO_2	~5	5.3921 (2)	156.77(2)
CNC	28.6017 32.4661 47.083 56.2998	111 200 220 311	1.5424 2.7821 2.5667 2.5008	CeO_2	~4	5.4014 (3)	157.58 (2)

* **Lattice parameter of standard CeO_2 for reference**

The Ni doping may be influence the microstructure of the powders. The XRD peak intensities as well as peak broadening of CNB and CNC samples showed, they may have smaller crystallite size than that of the

CNA. The calculated crystallite size of the samples was tabulated in Table.2. It is found to be the crystallite size of CNA has ~27nm, whereas the crystallite size of CNB and CNC decreased to less than 10nm. The Ni addition sufficiently plays role in the distortion of crystal structure [26]

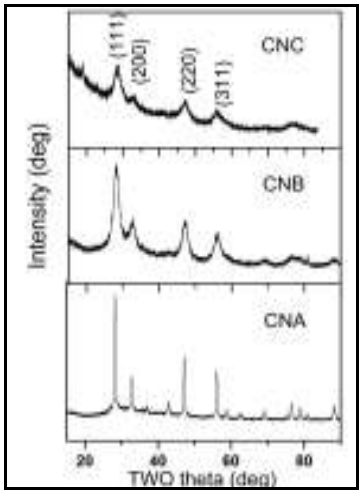

Fig 1 XRD pattern of Nickel doped nanocrystalline ceria

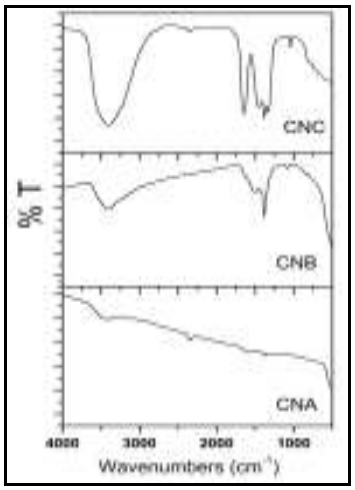

Fig. 2 FTIR spectrum of Nickel doped Ceria

Fig.2 shows FTIR spectrum of Nickel doped ceria nanocrystalline powder in the wave number range from 400 to 4000 cm^{-1}. Two peaks were shown at 3423 cm^{-1} and 2356 cm^{-1} in spectrum of CNA sample related to OH group contributed by water content and C-H Stretching mode of hydrocarbon. In CNB sample the absorption peak at 1503 cm^{-1} confirms the presence of unburned –COOH due to fuel content and peak at 1382 cm^{-1} indicates the symmetric N-O stretching vibration due to traces of nitrates. In CNC sample, the intense band at 3390 cm^{-1} and 1647 cm^{-1} corresponds to the stretching (O–H) mode of (H-bonded) water molecules, and bending vibration of (OH), respectively. The band around 1042 cm^{-1} is due to C-O alkoxy bond from the combustion components.

Fig.3 shows UV-Vis spectrum of nickel doped ceria nanocrystalline powder. It was observed that, enhanced absorption in the visible region was present at the UV-Vis spectrum. Hence Nickel doped ceria nanocrystalline material has the ability to absorb light in the visible region. The band gap of the powders were determined [27,28] from the cut off wavelength.

Table 3 Band gap value of Nickel doped ceria

Sample	λm	E Jouls	Bandgap energy (eV)
CNA	4.00E-07	4.97E-19	3.1
CNB	5.80E-07	3.43E-19	2.14
CNC	8.00E-07	2.48E-19	1.55

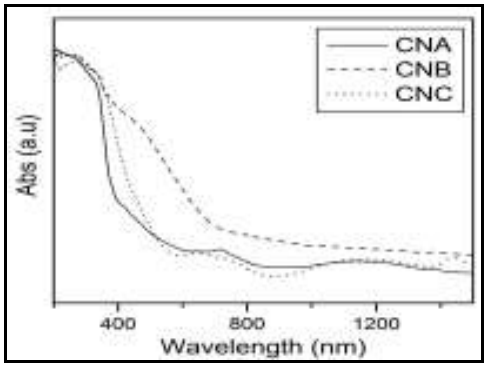

Fig. 3 UV-Vis spectrum of Nickel doped Ceria

The extended absorption of doped ceria up to the visible region was due to formation of vacancies also to the advent of Ce^{3+} ions or one Ce^{4+} is replaced by two Ni^{2+}. There is no sharp absorption edge exist in the samples due the doping of Nickel. Two absorption edges were observed in CNA a sample, which corresponds to Ni-doped ceria and NiO. Whereas the CNB also shows two absorption edges, but not very sharp, may be due to the absorption edges belongs to Ni-doped ceria and very small amount of excessive NiO. The NiO content may be less than 5 volume percent in the sample, due to this, the XRD of CNB didn't show any peaks corresponds to NiO. The CNC sample absorption edges clearly indicates only one absorption edges, belongs to Ni-doped ceria. Low band gap energy due to more number of Ni was dispersed on the ceria lattice, therefore more grain boundaries were noted in SEM images. The changes of the absorption edge are due to the concentration of nickel content. The higher concentration of grain boundaries is responsible for broadening the absorption edge and the apparent shift toward lower energies of the band gap [29]. The band gap values show the concentration of Ni dispersed on ceria lattice. In CNA sample, less number of Ni was dispersed due to limit of solubility, thereby bandgap value was good agreement with reported value of pure ceria. In CNB sample, concentration of Ni dispersed on the surface is more than the concentration of ceria but in CNC sample the concentration of ceria is more than Ni which further increase the band gap value. Due to increase of lattice parameter may build it easier for Ni atoms to go through the lattice, thus enhancing the interaction between Ni and ceria.

SEM images captured structural morphology and microstructure of Nickel doped nanocrystalline Ceria is shown in Fig.4. As prepared nanocrystalline powders was agglomerated due to rate of reaction during preparation process in CNA and CNB samples. In CNA samples shown two different grain boundaries as per the results obtained in XRD and UV-Vis spectrum. But the morphology of CNC sample indicates the formation of well-defined grain boundary with distorted cubic structure of ceria. The prepared nanocrystalline powder was agglomerated, making it difficult to discriminate individual crystallites exhibits clear lattice fringes observed in TEM images visualized in Fig.5. The observed fringes may due to the lattice distortion by the substitution of Ni in the FCC lattice. Ceria powders prepared at any conditions lead to the formation of particle agglomerated due to van der Walls forces responsible for the formation of ultra-fine ceria particles [29]. Presence of bright white ring on the SAED pattern indicates that the crystallinity of the Ni-doped ceria.

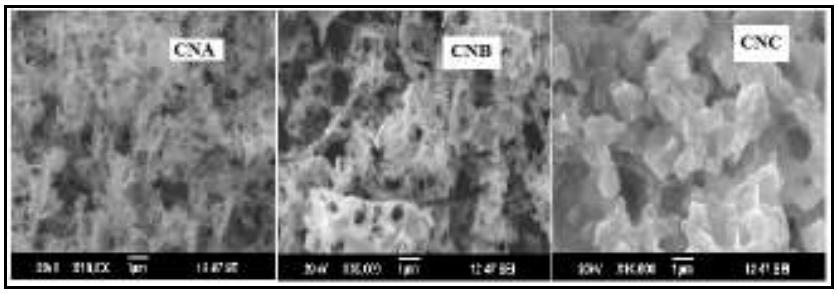

Fig: 4 SEM images of nickel doped nanocrystalline ceria

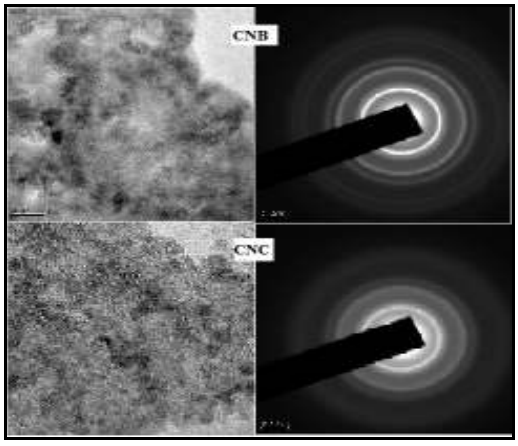

Fig: 5 TEM and SAED images of nickel doped nanocrystalline ceria

Conclusion:

Nickel doped ceria nanocrystalline samples were successfully prepared by microwave combustion technique using glycine and sorbitol as fuels. The prepared powders were characterized for phase purity and crystal structure parameters by X-ray diffraction. Three different Ni/Ce ratio compositions of powders were synthesized. It is observed that the Ni/Ce ratio play the role for the phase pure Ni-doped ceria or the segregation of NiO phase. Ni-doping was confirmed from their structural parameters such as lattice "a" and unit cell volume changes of the powders. Also the ratio of Ni/Ce will play the major role in the reduction of crystallite of the prepared powder in the nano meter level. Surface morphology of the powders also well agrees with the X-ray diffraction results. TEM studies also suggested the powders were polycrystalline. The optical studies (UV-Visible and FTIR) also confirm the purity of the powders and spectral band gap of the Ni-doped ceria. It is confirmed the optical band gap value of Ni-doped ceria was highly affected by the concentration of Ni dispersed in ceria lattice. From these studies it is confirmed the concentration CNB is optimized composition for getting good quality Ni-doped nano ceria.

References

1. Ashok Kumar Baral, Sankaranarayanan, V., "Ionic Transport Properties in Nanocrystalline $Ce_{0.8}A_{0.2}O_{2-d}$ (with A = Eu, Gd, Dy, and Ho) Materials", Nanoscale Res Lett , 2010, 5; 637–643.
2. Liangdong Fan, Guoquan Zhang, Mingming Chen, Chengyang Wang, Jing Di, Bin Zhu, "Proton and Oxygen Ionic Conductivity of Doped Ceria-Carbonate Composite by Modified Wagner Polarization", Int. J. Electrochem. Sci., 2012, 7; 8420 – 8435.
3. Mogens Mogensen , Nigel M., Sammes, Geoff A., Tompsett, "Physical, chemical and electrochemical properties of pure and doped ceria", Solid State Ionics, 2000, 129, 63–94,
4. Hilaire,S., Wanga, X., Luoa, T., Gorte, R,J., Wagner, J., "A comparative study of water-gas-shift reaction over ceria supported metallic catalysts", Applied Catalysis A: General, 2001,215; 271–278.
5. Mangalaraja R.V, Ananthakumar.S, Kasimayan Uma, Romel M, Jimenez, Marta Lopez Carlos. P,Camurri,"Microhardness and fracture toughness of $Ce_{0.9}Gd_{0.1}O_{1.95}$ for manufacturing solid oxide electrolytes" Mater.Sci.Eng A, 2009, 517; 91-96.
6. Qi Fu, Steven Fiore, Howard Saltburg, Xiaomei Qi and Maria Flytzani-Stephanopoulos, "Nanocrystalline ceria based catalysts for water-gas shift", Fuel chemistry Division preprints 2002, 47 ; 605.
7. Rui Si, Ya-Wen Zhang, Chao-Xian Xiao, Shi-Jie Li, Bing-Xiong Lin, Yuan Kou and Chun-Hua Yan " Non-template hydrothermal route derived mesoporous $Ce_{0.2}Zr_{0.8}O_2$ nanosized powders with blue shifted UV absorption and high Co conversion activity", Phys,Chem.Chem.Phys, 2004, 6; 1056-1063.
8. E.M. Logothetis, Proceedings of the 12th State of-the-Art Symposium on Ceramics in Service of Men, Washington, DC, 1976.
9. Jianqiang Wang, Meiqing Shen, Jun Wang, Ming Yang, Wulin Wang, Jie Ma, Liwei Jia, Effect of Ni-doping of ceria based materials and their micro-structures and dynamic oxygen storage and release behaviors, Catt.Lett., 2012, 140; 38-48.
10. Xian Cunni, Wang Shaofei, Sun Chunwen, Li Hong, Chan Suiwai & Chen Liquan*, Chinese Journal of Catalysis*, 2013**,** 34; 305–312.
11. Komandur V.R. Chary, Pendyala Venkat Ramana Rao, V. Vishwanathan, "Synthesis and high performance of ceria supported nickel catalysts for hydrodechlorination reaction",Catalysis Communications, 2006**,** 7; 974–978.
12. P. V. Aravind, J. P. Ouweltjes, N. Woudstra and G. Rietveld, "Impact of Biomass-Derived Contaminants on SOFCs with Ni/Gadolinia-Doped Ceria Anodes", Electrochemical and Solid-State Letters, 2008, 11; B24-B28.
13. Deryn Chu, & Ivan C. Lee, Proceedings for the Army Science Conference (24th) Held on 29 November – 2 December 2005 in Orlando, Florida.
14. Liu Yongmei, Cao Yong, Fan Kangnian, A Novel CeNiO Naonocomposite System For Low Temperature Oxidative Dehydrogenation of Propane, http://www.paper.edu.cn
15. S. T. Aruna, V. K. William Grips, V. Ezhil Selvi and K. S. Rajam, Studies on electrodeposited nickel–yttria doped ceria composite coatings, J Appl Electrochem., 2007**,** 37; 991–1000.
16. O. Yildiz. A.M. Soydan, A. Ata, B. Tunaboylu, D. Akin and E.F. Pcizade, Properties of Ceria Based Novel Anode Nanopowders Synthesized by Glycine-Nitrate Process, ACTA PHYSICA POLONICA A, 2013, 123; 432-435.

17. Ranjan K. Pati, Ivan C. Lee, Sicong Hou, Osifo Akhuemonkhan, Karen J. Gaskell, Qi Wang, Anatoly I. Frenkel, Deryn Chu, Lourdes G. Salamanca-Riba, and Sheryl H. Ehrman, Flame Synthesis of Nanosized Cu-Ce-O, Ni-Ce-O, and Fe-Ce-O Catalysts for the Water-Gas Shift (WGS) Reaction, Applied materials and interfaces, 2009, 1; 2624-2635.
18. Kuo-Hsin Lin, Cheng-You Tsai, Alex C. C. Chang, Preparation of High Surface Area Mesoporous $Ni_{2x}Ce_{1-x}O_2$ (x = 0, 0.05, 0.13, 0.2) and Its Applications in Methane Steam Reforming, Modern Research in Catalysis, 2013, 2; 42-49.
19. Lanlin Zhang, Preparation of multi-component ceramic nanoparticles, 2004, www.mse.eng.ohio-state.edu/fac_staff/faculty/verweij
20. V.K. Saxena and Usha Chandra, Microwave Synthesis: A Physical Concept, www.intechopen.com
21. Warren, B. E. 1990. X-ray diffraction. Dover Publications, New York.
22. Klug H P & Alexander L E, 1954, X-ray diffraction procedures, (New York: Wiley).
23. Holland T J B & Redfern S A T, *Mineralogical Magazine*, 61, 1997, 65.
24. Wolcyrz M & Kepinski L, *J Solid State Chem*, 99, 1992, 409. (Standard Lattice).
25. Laura Barrio, Ania Kubacka, Gong Zhou, Michael Estrella, Arturo Martinez-Arias, Jonathan C. Hanson, Marcos Fernandez-Garcia, and Jose A. Rodriguez, Unusual Physical and Chemical Properties of Ni in $Ce_{1-x}Ni_xO_{2-y}$ Oxides: Structural Characterization and Catalytic Activity for the Water Gas Shift Reaction, J. Phys. Chem. C, 2010, 114; 12689–12697.
26. Jianqiang Wang, Meiqing Shen, Jun Wang, Ming Yang, Wulin Wang, Jie Ma, Liwei Jia, Effect of Ni-doping of ceria based materials and their micro-structures and dynamic oxygen storage and release behaviors, Catt.Lett., 2012, 140; 38-48.
27. Hoffman, M, Martin S, Choi W, & Bahnemann D, Chemical Review, 95, 1995, 69.
28. An Investigation of TiO_2-$ZnFe_2O_4$ Nanocomposites for Visible Light Photo catalysis by Jeremy Wade, A thesis submitted to Department of Electrical Engineering; College of Engineering, University of South Florida, March 24, 2005**.**
29. M.L. Dos Santos, R.C. Lima, C.S. Riccardi, R.L. Tranquilin, P.R. Bueno, J.A.Varela, E. Longo, Preparation and characterization of ceria nanosphere by microwave-hydrothermal method, Materials Letters, 2008, 62; 4509-4511.

*****